Carbohydrate Polymers 90 (2012) 1273–1280

Contents lists available at SciVerse ScienceDirect

Carbohydrate Polymers

journal homepage: www.elsevier.com/locate/carbpol

Regioselective fluorescent labeling of *N*,*N*,*N*-trimethyl chitosan *via* oxime formation

Berglind E. Benediktsdóttir[a], Kasper K. Sørensen[b], Mikkel B. Thygesen[b], Knud J. Jensen[b], Thórarinn Gudjónsson[c], Ólafur Baldursson[d], Már Másson[a,*]

[a] Faculty of Pharmaceutical Sciences, School of Health Sciences, University of Iceland, Hofsvallagata 53, IS-107 Reykjavik, Iceland
[b] Center for Carbohydrate Recognition and Signaling, Faculty of Science, Department of Chemistry, University of Copenhagen, Thorvaldsensvej 40, DK-1871 Fredriksberg C, Copenhagen, Denmark
[c] Biomedical Center, School of Health Sciences, University of Iceland, Vatnsmýrarvegur 16, IS-101 Reykjavik, Iceland
[d] Department of Pulmonary Medicine, Landspitali – The National University Hospital of Iceland, Eiríksgata 5, IS-101 Reykjavik, Iceland

ARTICLE INFO

Article history:
Received 13 April 2012
Received in revised form 14 June 2012
Accepted 23 June 2012
Available online 1 July 2012

Keywords:
N,*N*,*N*-trimethyl chitosan
Fluorescence
Polysaccharide
Molecular weight
Oxime

ABSTRACT

Fluorescent labeling of chitosan and its derivatives is widely used for *in vitro* visualization and is accomplished by random introduction of the fluorophore to the polymer backbone, conceivably altering the bioactivity of the polymer. Here, we report for the first time the regioselective conjugation of a fluorophore to the reducing end of a fully *N*,*N*,*N*-trimethylated chitosan (TMC) by oxime formation. End-labeled conjugation of 5-(2-((aminooxyacetyl)amino)ethylamino)naphthalene-1-sulfonic acid (EDANS-O-NH_2) fluorophore to TMC to form TMC-oxime-EDANS (f-TMC) was confirmed by ^{1}H NMR and fluorescence spectroscopy. Average molecular weight calculations of f-TMC with ^{1}H NMR and fluorescence spectroscopy gave similar results or ~7.7 kDa. f-TMC in human bronchial epithelial cells was both cell membrane bound as well as intracellularly localized. This demonstrates the proof-of-concept for selective oxime formation at the reducing end of a chitosan derivative, which can be used for tracking chitosan in gene and drug delivery purposes and gives rise to further modifications with other functional groups.

1. Introduction

Chitosan has been studied as a paracellular permeation enhancer for hydrophilic molecules (Artursson, Lindmark, Davis, & Illum, 1994) and macromolecules (Illum, Farraj, & Davis, 1994; Şenel et al., 2000) by altering tight junction expression (Schipper et al., 1997; Yeh et al., 2011). Various other applications have also been investigated which include stimulation of cell differentiation and growth (Mathews, Gupta, Bhonde, & Totey, 2011; Muzzarelli, 2009; Muzzarelli, Greco, Busilacchi, Sollazzo, & Gigante, 2012) and use as an antimicrobial agent (Rabea, Badawy, Stevens, Smagghe, & Steurbaut, 2003). However, practical use of chitosan is limited due to poor aqueous solubility at physiological pH values. Consequently, quaternized chitosan derivatives, such as fully *N*,*N*,*N*-trimethylated chitosan (TMC) (Benediktsdóttir et al., 2011) and trimethylated-6-amino-6-deoxy chitosan (Sadeghi et al., 2008) have been synthesized in order to enhance aqueous solubility and biological activity.

Since early reports of synthesis of fluorescein isothiocyanate (FITC) labeled chitosan (Onishi & Machida, 1999; Qaqish & Amiji, 1999), studies focused on visualizing the FITC-labeled chitosan *in vitro* have revealed that chitosan in solution usually adhere to the cellular membrane and chitosan nanoparticles are taken up by the cells (Huang, Ma, Khor, & Lim, 2002; Jia, Chen, Xu, Han, & Xu, 2009). In addition to FITC, other fluorophores have been randomly introduced to the amino group of chitosan, such as lissamine–rhodamine (Schipper et al., 1997) and Cy5.5 conjugated to glycol modified chitosan (Nam et al., 2010). Reports of structure characterization of these fluorescently labeled chitosan derivatives have been scarce. Incorporating these fluorophores randomly into the chitosan backbone has become a widely used application to visualize the localization of the polymer *in vitro*. However, this introduction could have some effects on the spatial structure of the polymer thereby possibly altering its biological properties (Fei & Gu, 2009). The size distribution of fluorescent chitosan nanoparticles formed can also be affected (Huang, Khor, & Lim, 2004). Furthermore, these random labeling techniques utilize the free amino group on the polymer backbone and are therefore not applicable to chitosan derivatives, such as TMC, where the amino group is blocked by methylation. In contrast, the reducing end of TMC provides a unique chemical functionality for appending a fluorophore with high regioselectivity, provided that reagents and conditions can be developed for reactions at this masked aldehyde moiety. The aminooxy group is highly reactive towards carbonyl groups,

* Corresponding author. Tel.: +354 525 4463; fax: +354 525 4071.
E-mail address: mmasson@hi.is (M. Másson).

0144-8617/$ – see front matter © 2012 Elsevier Ltd. All rights reserved.
http://dx.doi.org/10.1016/j.carbpol.2012.06.070

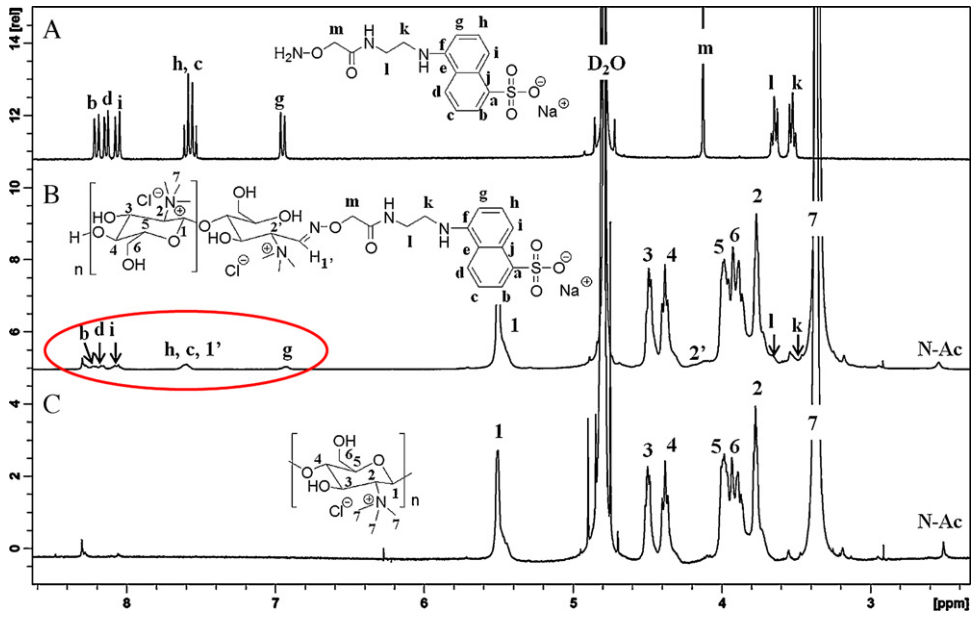

Fig. 1. ^{1}H NMR spectra: (A) EDANS-O-NH_2. (B) f-TMC (TMC-oxime-EDANS) with EDANS conjugation marked with circle. (C) TMC.

such as aldehydes and ketones (Langenhan & Thorson, 2005) and could therefore be used for oxime conjugation between the reducing end of TMC and an aminooxy linked fluorophore. Since such conjugation is highly selective, it could be used to determine the resulting molecular weight of the fluorescent polymer by ^{1}H NMR and fluorescent spectroscopy along with visualizing the location of TMC *in vitro*. To date, fluorescent labeling of TMC or other derivatives where the amino groups are completely blocked has not been reported.

2. Experimental

2.1. Materials

Chitosan HCl (G020102-1) with an average molecular weight (MW) of 8.1 kDa, as determined by end-reducing assay (Miller, 1959) and 8.5 kDa, as determined by viscometric methods (Ottoy, Varum, & Smidsrod, 1996) was provided by Genis EHF, Iceland. Degree of acetylation (DA) was estimated 0.03 according to ^{1}H NMR. All other chemicals and reagents were commercially available, of reagent grade or higher and used as received (Sigma–Aldrich, St. Louis, USA). Dialysis membrane (Spectra/Por, MW cutoff 3500 Da) and Float-A-Lyzer (Spectra/Por, MW cutoff 3.5–5.0 kDa, 5 ml sample volume) were purchased from Spectrum Laboratories Inc. (Rancho Dominguez, USA). LHC-9 cell culture medium was supplemented with penicillin and streptomycin (Gibco, Life Technologies, NY, USA). Fetal bovine serum (FBS) was obtained from Gibco (Life Technologies, NY, USA). Chambered culture slides and other cell culture plastics were purchased from BD Falcon (Bedford, MA, USA). Hanks Balanced Salt solution (HBSS) containing NaCl (146.94 mM), KCl (5.37 mM), Na_2HPO_4 (0.34 mM), KH_2PO_4 (0.44 mM), $CaCl_2{\cdot}2H_2O$ (1.80 mM), $MgSO_4$ (0.81 mM), $NaHCO_3$ (25 mM), D-glucose (5.55 mM) and HEPES (25 mM) was buffered at pH 7.4. Mouse monoclonal E-cadherin (IgG_{2a}) was purchased from BD Bioscience (NJ, USA) and Alexa Fluor 526 goat anti-mouse IgG_{2a}, was purchased from Invitrogen (Life Sciences, NY, USA). Fluoromount-G antifade solution was purchased from SouthernBiotech (Birmingham, USA).

2.2. Synthesis

2.2.1. N,N,N-trimethyl chitosan (TMC, **1**)

TMC homopolymer was synthesized according to our previous publication (Benediktsdóttir et al., 2011). In brief, chitosan HCl was stirred in methanesulfonic acid yielding chitosan mesylate salt. Introduction of the di-*tert*-butyldimethylsilyl protection groups was done by dissolving the mesylate salt in DMSO followed by addition of tert-butyldimethylsilyl chloride, forming di-TBDMS chitosan. Then, di-TBDMS chitosan was trimethylated with methyl iodide, deprotected with tetrabutylammonium fluoride and ion exchanged in NaCl solution yielding the final materal, *N,N,N*-trimethyl chitosan chloride (TMC). ^{1}H NMR (300 MHz, D_2O, Fig. 1C): δ ppm 2.08 (s, ~0.03H), 3.35 (s, 9H), 3.75 (s, 1H), 3.83–3.99 (m, 2H), 4.36 (t, 1H), 4.47 (t, 1H), 5.49 (s, 1H).

2.2.2. 5-(2-((Aminooxyacetyl)amino)ethylamino)naphthalene-1-sulfonic acid (EDANS-O-NH_2, **2**)

Synthesis of EDANS-O-NH_2 was carried out according to a previously published procedure (Takaoka, Tsutsumi, Kasagi, Nakata, & Hamachi, 2006) but with several modifications. 1,5-EDANS (266 mg, 1 mmol) was added to a solution of *N*-Boc-aminooxyacetic acid (291 mg, 1 mmol), *O*-benzotriazole-*N,N,N′,N′*-tetramethyluronium hexafluorophosphate (379 mg, 1 mmol), 1-hydroxy-benzotriazole hydrate (135 mg, 1 mmol) and *N,N′*-diisopropylethylamine (342 μL, 2 mmol) in dimethylformamide. The reaction was stirred at room temperature for 16 h. The product was purified using HPLC on a C18 column with a gradient from 5% to 30% acetonitrile in H_2O. The freeze-dried product was then dissolved in trifluoroacetic acid (TFA)/CH_2Cl_2 (1:1) and stirred for 2 h at room temperature to remove the Boc group. TFA and CH_2Cl_2 were removed by N_2. The resulting solid was then redissolved in water/acetonitrile (1:1) then freeze-dried to provide the title compound (276 mg, 81% for the two steps) as a white solid. ^{1}H NMR (300 MHz, D_2O, Fig. 1A): δ ppm 3.52 (t, J_H = 5.8 Hz, 2H), 3.65 (t, J_H = 5.7 Hz, 2H), 4.13 (s, 2H), 6.95 (d, J_H = 7.8 Hz, 1H), 7.56 (t, J_H = 7.5 Hz, overlapped, 1H), 7.59 (t, J_H = 7.8 Hz, overlapped, 1H), 8.06 (d, J_H = 8.6 Hz, 1H), 8.14 (dd, J_{H3} = 7.3 Hz, J_{H4} = 0.9 Hz, 1H), 8.20 (d, J_H = 8.7 Hz, 1H).

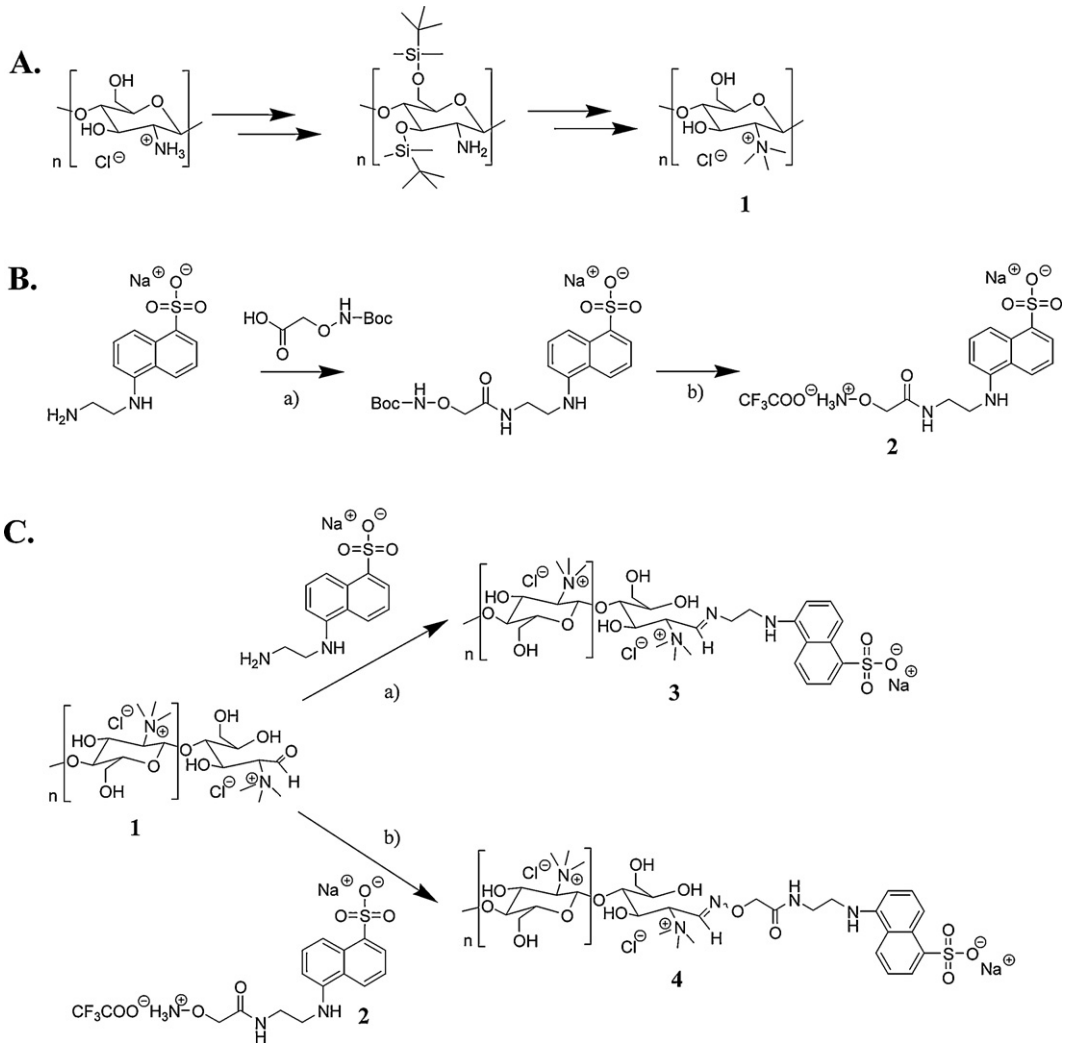

Scheme 1. Synthesis of *N,N,N*-trimethyl chitosan (TMC, **1**), EDANS-O-NH_2 (**2**), TMC-imine-EDANS (**3**) and TMC-oxime-EDANS (f-TMC, **4**)[a]. *Note:* [a]Reagents and conditions: (A) According to previous published procedure (Benediktsdóttir et al., 2011). (B) (a) *O*-benzotriazole-*N,N,N′,N′*-tetramethyluronium, 1-hydroxy-benzotriazole hydrate and *N,N′*-diisopropylethylamine in dimethylformamide at rt for 16 h. (b) Product from (a) was stirred in trifluoroacetic acid for 2 h at rt to produce EDANS-O-NH_2. (C) (a) EDANS, 100 mM aniline in 100 mM acetate buffer at pH 4.5, 50 °C. (b) EDANS-O-NH_2, 100 mM aniline in 100 mM acetate buffer at pH 4.5, 50 °C.

2.2.3. TMC-imine-EDANS (**3**)

TMC (36 mg) and 1,5-EDANS (7 mg) were stirred in 3 ml of acetate buffer (100 mM, pH 4.5) in the presence of aniline (100 mM), in a closed reaction vial, protected from light, at 50 °C for 72 h. The solution was then dialyzed in the dark against water for 24 h, then against 5% aq. NaCl solution for 24 h and finally against water for an additional 48 h (yield: 33 mg (92%)).

2.2.4. TMC-oxime-EDANS (f-TMC, **4**)

TMC (36 mg) and EDANS-O-NH_2 (7 mg) were dissolved in 3 ml acetate buffer (100 mM, pH 4.5) in the presence of aniline (100 mM) and stirred in a closed reaction vial, protected from light, at 50 °C for 72 h. The solution was dialyzed in the dark against water for 24 h, then against 5% aq. NaCl solution for 24 h and finally against water for additional 48 h (yield: 35 mg (98%)). ^{1}H NMR (400 MHz, D_2O, Fig. 1B): δ ppm 2.09 (s, ~0.03H), 3.35 (s, 9H), 3.53 (br m, ~0.06H), 3.65 (br m, ~0.06H), 3.76 (s, 1H), 3.88–3.92 (m, 1H), 3.99 (m, 1H), 4.12 (m, ~0.02H), 4.37 (t, 1H), 4.48 (t, 1H), 5.50 (s, 1H), 6.92 (br s, ~0.03H), 7.59–7.63 (br s, ~0.08H), 8.03–8.07 (m, ~0.03H), 8.16 (m, ~0.03H), 8.21 (m, ~0.03H).

2.3. Characterization

2.3.1. NMR

^{1}H NMR spectra were recorded with a Bruker Avance 300 MHz instrument and ^{1}H–^{1}H COSY and ^{13}C–^{1}H HSQC NMR spectra were recorded with a Bruker 500 MHz instrument with an Observe cryoprobe. Spectra were run without water suppression and D_2O was used as NMR solvent with sample concentrations ranging from 10 to 15 mg/ml. The spectra were calibrated to previously reported value for the trimethyl peak (3.35 ppm) (Benediktsdóttir et al., 2011). Measurements were obtained without water suppression. The number average molecular weight (Mn) was determined from the ^{1}H NMR data by end-group analysis. First, the ratio of EDANS-O-NH_2 protons on the end-group in TMC-oxime-EDANS ($D_{EDANS\text{-}O\text{-}NH2}$) was determined from ^{1}H NMR spectra (Fig. 1B) using the following equation:

$$D_{EDANS\text{-}O\text{-}NH_2} = \left(\frac{\int \text{H-g}}{\int \text{H-1}} \times \frac{\text{Theoretical number of protons in H-1}}{\text{Theoretical number of protons in H-g}}\right) = \left(\frac{\int \text{H-g}}{\int \text{H-1}} \times \frac{1}{1}\right) \quad (1)$$

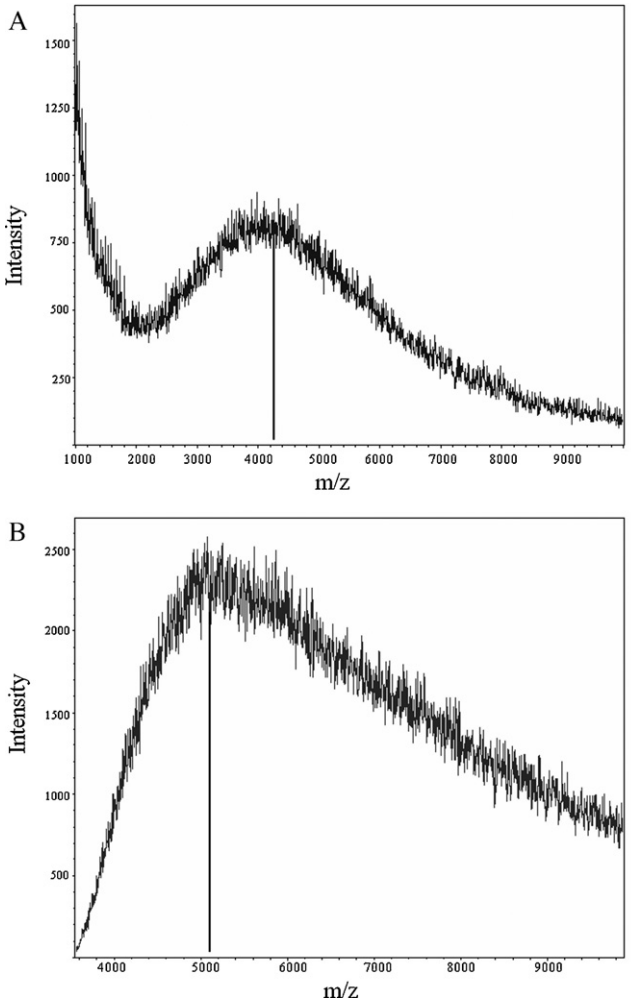

Fig. 2. MALDI-TOF of TMC determined in different matrixes: (A) Determined with α-cyano-4-hydroxycinnamic acid as the matrix. (B) Determined with 2,5-dihydroxybenzoic acid as the matrix.

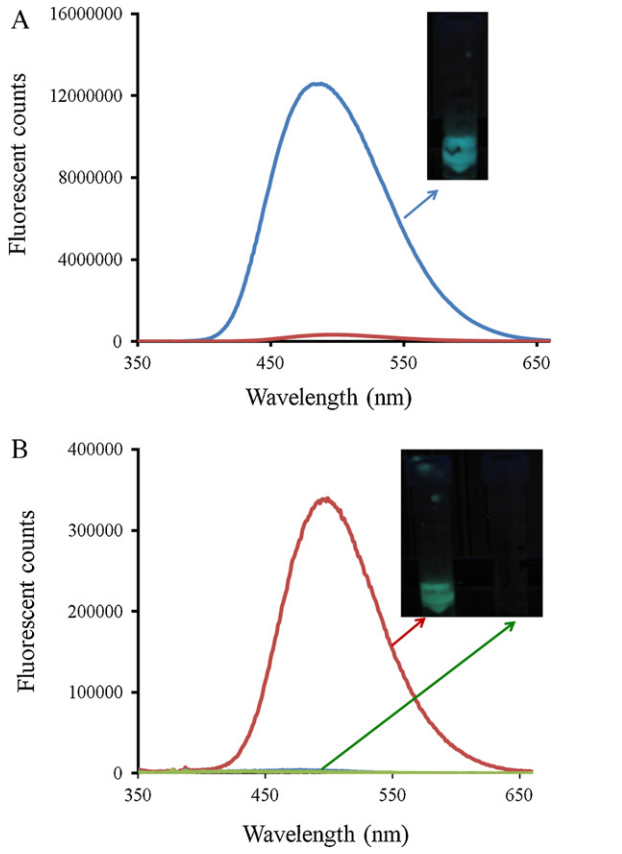

Fig. 3. Fluorescence emission spectra of EDANS and EDANS-O-NH_2 conjugated to TMC (f-TMC) in H_2O after excitation at 335 nm: (A) EDANS (blue) and f-TMC (red). (B) f-TMC (red), compound isolated after reaction between TMC and EDANS (green) and TMC (blue). (For interpretation of the references to color in this figure legend, the reader is referred to the web version of the article.)

where numbering of protons H-g (from EDANS-O-NH_2) and H-1 (from TMC) is according to Fig. 1B. Ratio of TMC units in TMC-oxime-EDANS (D_{TMC}) was then determined with the following equation:

$$D_{TMC} = 1 - D_{EDANS\text{-}O\text{-}NH_2} \quad (2)$$

Mn of TMC-oxime-EDANS was determined using the following equations:

$$\text{Number of TMC repeating units} = \frac{D_{TMC}}{D_{EDANS\text{-}O\text{-}NH_2}} \quad (3)$$

$$MW_{TMC\text{-}oxime\text{-}EDANS} = (\text{Number of TMC repeating units} \times MW_{\text{one TMC unit}}) \quad (4)$$

2.3.2. Fluorescence spectrometry

Fluorescence intensity was measured using a Spex FluoroMax at 22 °C with excitation wavelength of 335 nm. Each spectrum is the average of three accumulations. Equal amount of samples (mg/ml) in water was measured to enable direct comparison of fluorescence intensity. Calibration curve of EDANS fluorescence ($0.18–195 \times 10^{-6}$ M) was measured using fluorescence plate reader (Tecan GENios microplate reader, Männedorf, Switzerland) with excitation filter of 360 nm and emission filter of 535 nm. The calibration curve was used to calculate $D_{EDANS\text{-}O\text{-}NH2}$ and then Eqs. (2)–(4) were used to calculate the average MW of TMC-oxime-EDANS.

2.3.3. MALDI-TOF MS

Mass spectra were obtained using Microflex time-of-flight mass spectrometer (Bruker, Bremen, Germany). Spectra were collected in positive ion mode with 100 laser shots summed to produce the final spectrum. Measurements were done without baseline correction. Either 2,5-dihydroxybenzoic acid or α-cyano-4-hydroxycinnamic acid was used as the matrix (10 mg/ml). 1 μl of the matrix was mixed on a steel target plate with 1 μl of the TMC (1 mg/ml) and allowed to air-dry at room temperature.

2.4. In vitro studies

2.4.1. Culture of VA10 cells and visualization of f-TMC (4) in the epithelium

The bronchial cell line VA10 (Halldorsson et al., 2007) was used to study the location of f-TMC (**4**) in the epithelium with unmodified EDANS and the hypothetical TMC-imine-EDANS (**3**) as controls. The cells were cultured in LHC-9 medium and used between passages 17–21 and maintained at 37 °C in a humidified atmosphere of 95% air and 5% CO_2. Cells were seeded at a density of 7×10^5 cells/cm^2 on chambered culture slides and cultured until confluent. The monolayers were treated with either 0.5 mg/ml of f-TMC, 0.5 mg/ml of the hypothetical TMC-imine-EDANS or 0.0026 mg/ml of EDANS (similar amount of fluorescent units per ml buffer as in f-TMC)

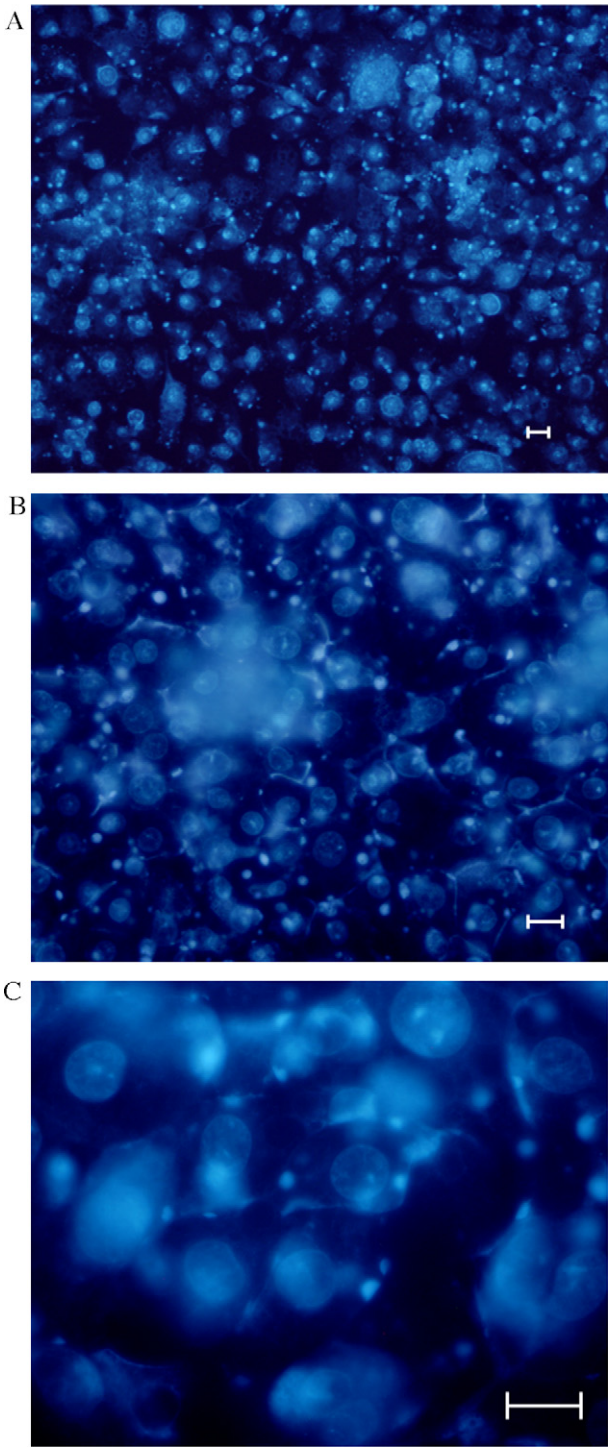

Fig. 4. Fluorescent microscopy images of VA10 cells in monolayer after incubation with f-TMC. (A) Incubation for 20 min at 37 °C. (B) Incubation for 2 h at 37 °C (40× magnification) and (C) (100× magnification); bar = 10 μm.

in HBSS buffer for 2 h. Subsequently, the monolayers were rinsed three times with prewarmed HBSS, fixed with 3.7% formaldehyde in PBS (pH 7.4) for 10 min and fluoromount-G added before visualization. For co-staining with E-cadherin, the monolayer was permeabilized after fixation with 0.1% Triton X-100/PBS for 7 min and blocked in 10% FBS in PBS for 10 min at room temperature. Subsequently, the monolayer was incubated with primary antibody against E-cadherin (1:125) for 30 min at room temperature followed by incubation with Alexa Fluor secondary antibody (1:1000) for 30 min and fluoromount-G added. All images were obtained with an epi-fluorescent microscope with matching filters (Nicon Eclipse-800) and photographed with Nikon DXM1200F digital camera.

2.4.2. Uptake studies in VA10 epithelial cells

VA10 cells, between passages 19–20, were seeded at a density of 2.1×10^4 cells/cm^2 on 12 well cell culture plates and cultured in LHC-9 until confluent. The cell monolayers were treated with either 0.0026 mg/ml EDANS in HBSS or 0.5 mg/ml f-TMC (**4**) in HBSS for 2 h. The uptake was terminated by washing the monolayers three times with ice-cold HBSS. Fluorescence of the cell lysate, obtained by applying 300 μl of 2% SDS solution (pH 8) to each well, was measured using fluorescence plate reader (Tecan GENios microplate reader, Männedorf, Switzerland) with excitation filter of 360 nm and emission filter of 535 nm. Protein concentration of the cell lysate was determined using the Bradford assay. Uptake was expressed as the quantity of f-TMC or EDANS (μg) present in 1 mg of protein (Mean ± SD, $n = 3$–4). The uptake results were compared with unpaired, two tailed Student's *t*-test (GraphPad Prism, GraphPad Software Inc., CA, USA) with $p < 0.05$ considered as statistical significant.

3. Results and discussion

3.1. Synthesis of fluorescently end-labeled N,N,N-trimethyl chitosan (f-TMC)

The reducing end of the TMC homopolymer (**1**, Scheme 1A) was conjugated with an aminooxy functionalized 5-((2-aminoethyl)amino)naphthalene-1-sulfonic acid (**2**, EDANS-O-NH_2, Scheme 1B) fluorophore forming TMC-oxime-EDANS (**4**, f-TMC, Scheme 1C). This can be seen by signals in the aromatic region of the ^{1}H NMR spectra assigned to the naphthalene moiety of the fluorophore (Fig. 1B). Conjugation of EDANS-O-NH_2 to TMC was estimated to result in an upfield shift of the methylene aminooxy protons (H-m), thereby localizing them under the H-5 and H-6 peaks of TMC. The amino ethylene protons in the fluorophore (H-k and H-l) were located in the same region as the TMC protons, making their existence barely detectable. However, the ^{1}H–^{1}H COSY revealed a correlation confirming their existence at 3.65 and 3.53 ppm (Fig. A.1A). Ring-chain tautomerism of oxime glycan conjugates (Finch & Merchant, 1975) such as the end-labeled TMC-oxime reduces the chance of observing the H-1′ peak in the ^{1}H NMR spectra. The major (E)-oxime tautomer form of H-1′ should appear at approx. 7.6 ppm (Jiménez-Castells, de la Torre, Andreu, & Gutiérrez-Gallego, 2008; Novoa-Carballal & Muller, 2012; Thygesen, Sauer, & Jensen, 2009), at the same place as aromatic protons from EDANS-O-NH_2. Due to the low intensity of the H-1′ peak, the correlation signals, to this peak, in COSY and HSQC NMR were weak and near the detection limit. However, from analysis of the ^{1}H–^{1}H COSY NMR spectra the H-1′ was found to appear at 7.63 ppm, showing a correlation to H-2′ at 4.12 ppm (Fig. A.1B). In addition, correlation between the H-1′ signal and the C-1′ signal at 152 ppm was observed in ^{13}C–^{1}H HSQC NMR spectra (Fig. A.1D), further supporting the oxime conjugation.

The attempted reaction between TMC and the amino group of EDANS did not provide a conjugate (the hypothetical imine **3**) since ^{1}H NMR data was consistent with the unmodified TMC (**1**, data not shown), thereby indicating very low efficiency in end-labeling. This is likely due to relative instability of the imine bond (Layer, 1963) compared to the oxime bond that has been reported to be relatively hydrolytically stable in aqueous solutions (Kalia & Raines, 2008). Consequently, the aminooxy group presents a more suitable approach for covalent linkage at the reducing end of TMC, compared

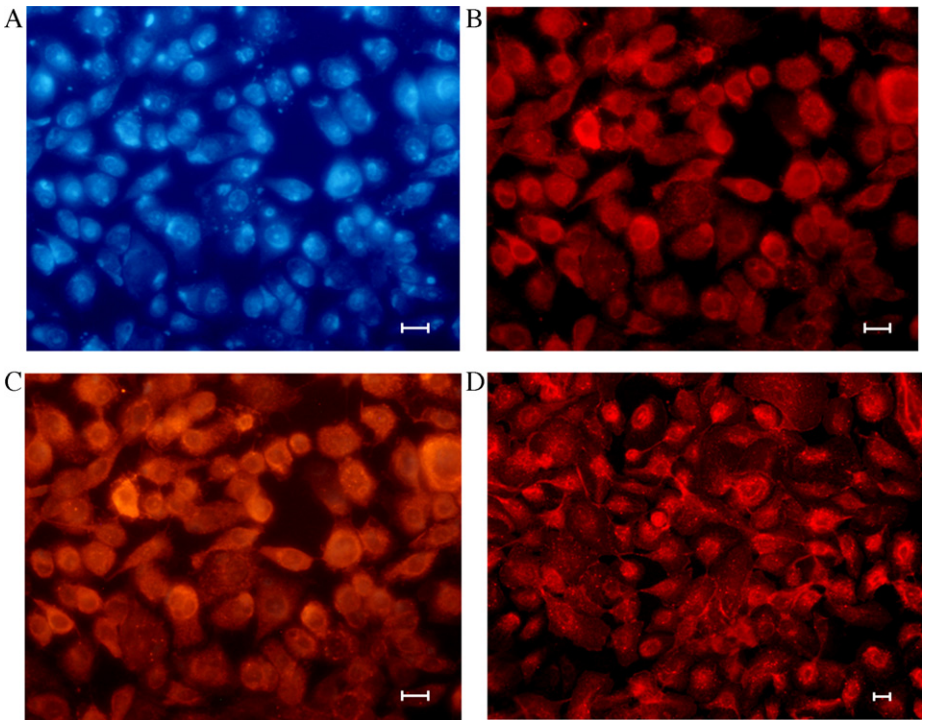

Fig. 5. Fluorescent microscopy images of VA10 cells in monolayer. (A) After incubation with 0.5 mg/ml f-TMC (366 nm) for 2 h at 37 °C. (B) Immunofluorescence staining for E-cadherin (526 nm) of the same section as shown in A. (C) Co-localization of f-TMC and E-cadherin. (D) Immunofluorescence staining for E-cadherin (526 nm) in non-treated cells; bar = 10 μm.

to an amino group, under current reaction conditions. The covalent linkage is shown by the peak-broadening of the fluorophore in the ^{1}H NMR spectra of f-TMC (Fig. 1B) and it is further supported by the observation from NMR that the dialysis procedure provides an f-TMC conjugate with approx. 1:1 molar ration between the polymer and the fluorophore.

The water soluble EDANS was chosen as a proof-of-concept fluorophore. It has a relatively long fluorescence lifetime and has effectively been used as a fluorescent donor in fluorescence energy transfer of EDANS/DABCYL (Matayoshi, Wang, Krafft, & Erickson, 1990). For this application, EDANS has been conjugated, *via* intermediate imine formation, through a glycosylamide linkage to the reducing end of chitopentaose for analyzing enzyme activity (Cottaz, Brasme, & Driguez, 2000). Chitosan can be functionalized at the reducing-end with an amino group and this has been utilized to minimize the degradation of the polymer (Muzzarelli, Terbojevich, Muzzarelli, & Francescangeli, 2002). The fact that the reducing end of TMC could be fluorescently labeled reflects the efficiency of the di-*tert*-butyldimethylsilyl protection strategy used to protect all hydroxyl groups of chitosan in the previous trimethylation step (Benediktsdóttir et al., 2011).

Chemoselective oxime formation has been used in glycochemistry to conjugate reducing glycans to gold nanoparticles (Thygesen, Sauer, et al., 2009; Thygesen, Sorensen, Clo, & Jensen, 2009) and microarrays (Cló, Blixt, & Jensen, 2010) and more recently to conjugate chitosan to poly(ethylene glycol) through the aminooxy linker (Novoa-Carballal & Muller, 2012). Oxime formation has also been utilized to conjugate *O*-benzyl aminooxy groups to the reducing end of glucose (Glc) and *N*-acetyl glucosamine (GlcNAc) (Thygesen et al., 2010). GlcNAc, the basic unit of chitin, has lower reactivity towards the aminooxy group compared to glucose (Lohse, Martins, Jørgensen, & Hindsgaul, 2006; Thygesen et al., 2010) showing that the substitution on the C-2 carbon affects the reactivity. The reducing end exists in equilibrium between the ring-closed hemiacetal, the open-chain aldehyde and most likely the hydrate as well. Since only the open chain aldehyde can react with the aminooxy group (Thygesen et al., 2010), the extent of ring opening affects the reactivity of oxime formation (Haas & Kadunce, 1962). Aniline (100 mM) has been reported to catalyze the oxime formation between *O*-benzyl aminooxy groups and GlcNAc (Thygesen et al., 2010) and was, therefore, used to catalyze the reaction of f-TMC combined with heating to 50 °C for 72 h to enable full conjugation. Although the presence of aniline (100 mM) as a catalyst has previously yielded up to 15% conversion to the *N*-phenyl-imine end-labeled glycan (Thygesen et al., 2010) we did not observe any peaks correlating to the *N*-phenyl group by NMR. However, low levels of *N*-phenyl-imine formation cannot be excluded as this would not have been detected in the NMR analysis of the carbohydrate polymer. The reaction was carried out in acetate buffer at pH 4.5, since glycan oxime formation proceeds with an optimum of pH 4–5 (Haas & Kadunce, 1962), at the pH where the aminooxy groups are partially neutral (Langenhan & Thorson, 2005).

3.2. Molecular weight determination of f-TMC

The end-group analysis of EDANS (*i.e.* ratio between EDANS and trimethyl glucosamine units) in f-TMC (**4**), calculated from ^{1}H NMR data (Fig. 1B and Eq. (1)), was 0.03. This data, assuming that all reducing ends were labeled, was used to calculate the number average MW (Mn) of f-TMC polymer of 7.75 kDa (Eqs. (2)–(4)). MALDI-TOF molecular weight measurements were also collected for the TMC polymer. Either 2,5-dihydroxybenzoic acid or α-cyano-4-hydroxycinnamic acid was used as a matrix and MALDI-TOF measurements gave peak MW of 4.2 kDa and 5.2 kDa respectively (Fig. 2). The linear ($r^2 \geq 0.99$) fluorescence calibration curve of EDANS was used to calculate the average MW of f-TMC (from Eq. (2–4)) and was found to be 7.74 kDa. Calculations from the NMR and fluorospectroscopy data give very similar values whereas MALDI-TOF gives a very crude average MW determination. Accordingly, it can be estimated that the molecular weight of f-TMC is around 7.7 kDa, which is a lower molecular weight than the starting chitosan (8.3 kDa).

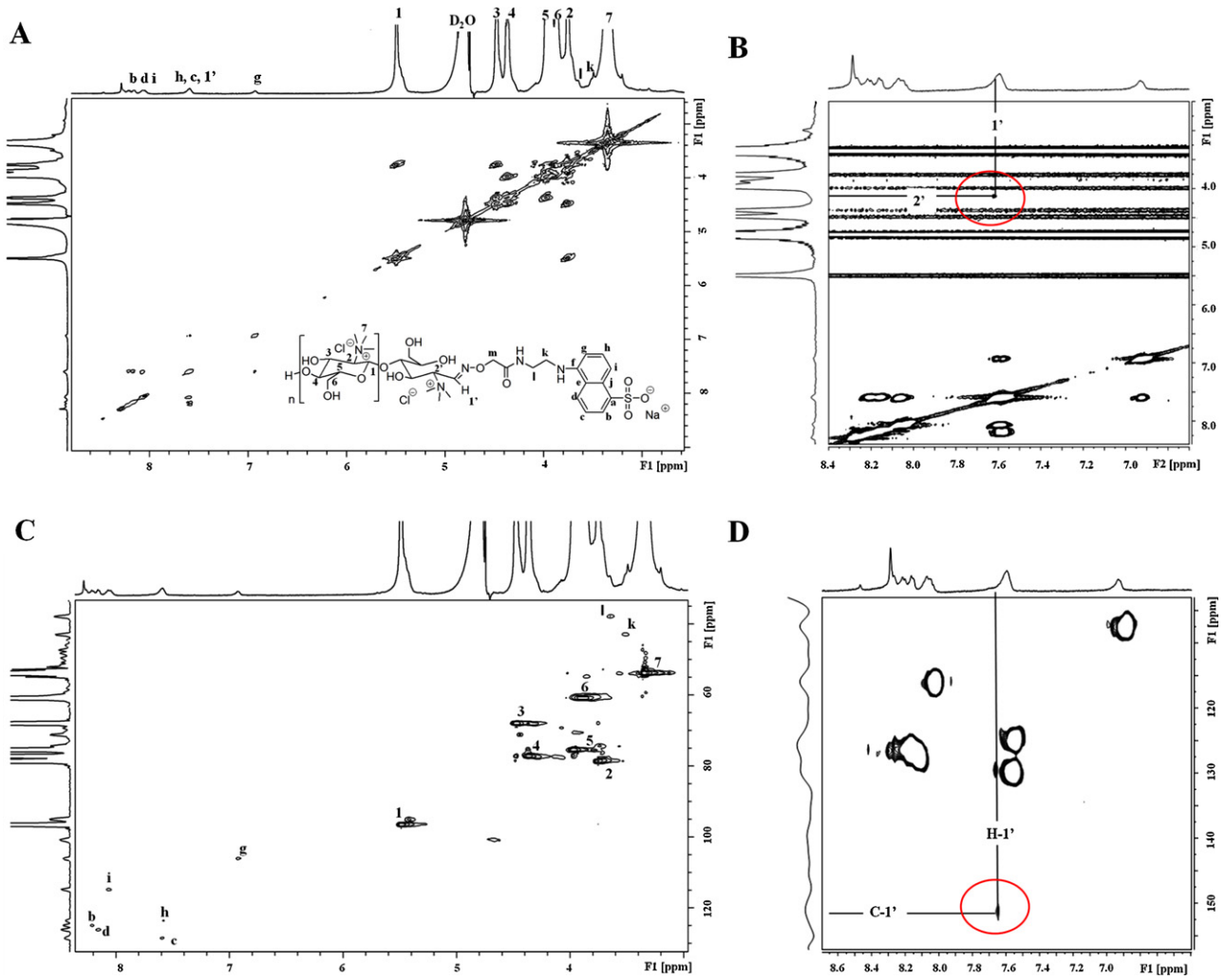

Fig. A.1. 2D NMR analysis of f-TMC. (A) ^{1}H–^{1}H COSY NMR spectra. (B) Enlarged COSY spectra showing the H-1′ to H-2′ correlation. (C) ^{13}C–^{1}H HSQC NMR spectra. (D) Enlarged HSQC spectra showing the correlation of H-1′ to C-1′.

3.3. Fluorescent properties of EDANS and f-TMC

Fluorospectrometric data showed that EDANS had λ_{em} 488 nm when excited at 335 nm (Fig. 3A). A similar fluorescence maximum, λ_{em} 499 nm, was observed for f-TMC (**4**) at the same excitation with much lower intensity than the fluorophore itself, which is to be expected for fluorescently end-labeled TMC (Fig. 3A and B). The attempted preparation of the hypothetical TMC imine derivative (**3**) did not provide a fluorescently labeled TMC (Fig. 3B) and was in accordance with the ^{1}H NMR data that also indicated that the conjugate did not form to any significant extent.

3.4. Visualization and uptake of f-TMC in bronchial epithelial cells

The fluorescent properties of f-TMC (**4**) were further explored in the VA10 bronchial epithelial cell line in order to establish the localization of the polymer (Halldorsson et al., 2007). The visualization was carried out using epi-fluorescent microscope since confocal scanning microscopy was not equipped to visualize the EDANS fluorophore. f-TMC (**4**, 0.5 mg/ml) was observed at the cell membrane as well as intracellularly (Fig. 4B and C) after only 20 min of incubation (Fig. 4A). No fluorescence was observed after incubation for 2 h with the hypothetical TMC-imine-EDANS (**3**) or with the EDANS fluorophore itself (data not shown) which further supports the reactivity and selectivity of the aminooxy group in the synthesis of f-TMC. Co-staining of f-TMC and the adherence junction protein E-cadherin (E-cad) showed intracellular localization of f-TMC and co-localization with E-Cad at the membrane surface (Fig. 5). Numerous articles have reported none or limited internalization of solubilized chitosan (Huang et al., 2004; Jia et al., 2009; Schipper et al., 1997). However, internalization of solubilized polyethylene glycol (PEG)-TMC copolymer has been described, with localization mainly in the perinuclear region of the cell when complexed with insulin (Mao et al., 2005). In addition, gene delivery studies have shown that TMC–DNA polyplexes are more efficiently internalized than chitosan–DNA polyplexes (Germershaus, Mao, Sitterberg, Bakowsky, & Kissel, 2008; Thanou, Florea, Geldof, Junginger, & Borchard, 2002) and that other cationic polymers, such as poly-L-lysine, are also effectively internalized (Ranaldi, Marigliano, Vespignani, Perozzi, & Sambuy, 2002). The cellular uptake study provided further confirmation of the internalization of f-TMC in the epithelial monolayer with significantly higher uptake ($p < 0.0001$) of f-TMC (32.01 ± 3.60 μg/mg protein) than EDANS control (0.073 ± 0.038 μg/mg protein). Since fluorescent microscopy shows that f-TMC is largely found intracellularly but also partially membrane bound, the amount detected in the uptake study contains both membrane bound and intracellularly localized f-TMC. Furthermore, these results show that the EDANS moiety of f-TMC does not contribute to the adhesion or internalization of the f-TMC polymer.

4. Conclusions

In this study, we report the first synthesis of a fluorescently labeled TMC obtained by highly regioselective oxime formation at the reducing end. Advantages of this novel approach include conjugation that should induce minimal structural changes to the chitosan backbone and fluorescent labeling that enables accurate molecular weight determination. In addition, this conjugation provides clear localization of the polymer *in vitro*, revealing localization both at the cell membrane as well as intracellularly. Selective oxime conjugation to the reducing end of TMC introduces new opportunities in chitosan chemistry. Besides allowing selective conjugation of other fluorophores, that offers numerous potential applications for gene- and drug delivery studies, this method also introduces the possibility of conjugating chitosan polymers to other functionally active moieties.

Acknowledgements

Financial support from the Icelandic Technology Development Fund, the Eimskip Fund of University of Iceland, the Bergthóru and Thorsteins Scheving Thorsteinssonar Fund and the University of Iceland Research Fund is gratefully acknowledged. We thank Kesara Anamthawat-Jónsson and Lilja Karlsdóttir at the Institute of Biology, University of Iceland for the help with fluorescent microscopy pictures.

References

Artursson, P., Lindmark, T., Davis, S. S., & Illum, L. (1994). Effect of chitosan on the permeability of monolayers of intestinal epithelial-cells (Caco-2). *Pharmaceutical Research*, *11*(9), 1358–1361.

Benediktsdóttir, B. E., Gaware, V. S., Rúnarsson, Ö. V., Jónsdóttir, S., Jensen, K. J., & Másson, M. (2011). Synthesis of *N,N,N*-trimethyl chitosan homopolymer and highly substituted *N*-alkyl-*N,N*-dimethyl chitosan derivatives with the aid of di-tert-butyldimethylsilyl chitosan. *Carbohydrate Polymers*, *86*(4), 1451–1460.

Cló, E., Blixt, O., & Jensen, K. J. (2010). Chemoselective reagents for covalent capture and display of glycans in microarrays. *European Journal of Organic Chemistry*, *2010*(3), 540–554.

Cottaz, S., Brasme, B., & Driguez, H. (2000). A fluorescence-quenched chitopentaose for the study of endo-chitinases and chitobiosidases. *European Journal of Biochemistry*, *267*(17), 5593–5600.

Fei, X., & Gu, Y. (2009). Progress in modifications and applications of fluorescent dye probe. *Progress in Natural Science*, *19*(1), 1–7.

Finch, P., & Merchant, Z. (1975). The structures of D-arabinose and D-glucose oximes. *Journal of the Chemical Society, Perkin Transactions*, *1*(17), 1682–1686.

Germershaus, O., Mao, S., Sitterberg, J., Bakowsky, U., & Kissel, T. (2008). Gene delivery using chitosan, trimethyl chitosan or polyethylenglycol-graft-trimethyl chitosan block copolymers: Establishment of structure–activity relationships in vitro. *Journal of Controlled Release*, *125*(2), 145–154.

Haas, J. W., & Kadunce, R. E. (1962). Rates of reaction of nitrogen bases with sugars. I. Studies of aldose oxime, semicarbazone and hydrazone formation. *Journal of the American Chemical Society*, *84*(24), 4910–4913.

Halldorsson, S., Asgrimsson, V., Axelsson, I., Gudmundsson, G., Steinarsdottir, M., Baldursson, O., et al. (2007). Differentiation potential of a basal epithelial cell line established from human bronchial explant. *In Vitro Cellular and Developmental Biology – Animal*, *43*(8), 283–289.

Huang, M., Khor, E., & Lim, L.-Y. (2004). Uptake and cytotoxicity of chitosan molecules and nanoparticles: Effects of molecular weight and degree of deacetylation. *Pharmaceutical Research*, *21*(2), 344–353.

Huang, M., Ma, Z., Khor, E., & Lim, L.-Y. (2002). Uptake of FITC-chitosan nanoparticles by A549 cells. *Pharmaceutical Research*, *19*(10), 1488–1494.

Illum, L., Farraj, N. F., & Davis, S. S. (1994). Chitosan as a novel nasal delivery system for peptide drugs. *Pharmaceutical Research*, *11*(8), 1186–1189.

Jia, X., Chen, X., Xu, Y., Han, X., & Xu, Z. (2009). Tracing transport of chitosan nanoparticles and molecules in Caco-2 cells by fluorescent labeling. *Carbohydrate Polymers*, *78*(2), 323–329.

Jiménez-Castells, C., de la Torre, B., Andreu, D., & Gutiérrez-Gallego, R. (2008). Neo-glycopeptides: The importance of sugar core conformation in oxime-linked glycoprobes for interaction studies. *Glycoconjugate Journal*, *25*(9), 879–887.

Kalia, J., & Raines, R. T. (2008). Hydrolytic stability of hydrazones and oximes. *Angewandte Chemie International Edition*, *47*(39), 7523–7526.

Langenhan, J. M., & Thorson, J. S. (2005). Recent carbohydrate-based chemoselective ligation applications. *ChemInform*, *36*(42), 59–81.

Layer, R. W. (1963). The chemistry of imines. *Chemical Reviews*, *63*(5), 489–510.

Lohse, A., Martins, R., Jørgensen, M. R., & Hindsgaul, O. (2006). Solid-phase oligosaccharide tagging (SPOT): Validation on glycolipid-derived structures. *Angewandte Chemie International Edition*, *45*(25), 4167–4172.

Mao, S., Germershaus, O., Fischer, D., Linn, T., Schnepf, R., & Kissel, T. (2005). Uptake and transport of PEG-graft-trimethyl-chitosan copolymer–insulin nanocomplexes by epithelial cells. *Pharmaceutical Research*, *22*(12), 2058–2068.

Matayoshi, E. D., Wang, G. T., Krafft, G. A., & Erickson, J. (1990). Novel fluorogenic substrates for assaying retroviral proteases by resonance energy-transfer. *Science*, *247*(4945), 954–958.

Mathews, S., Gupta, P. K., Bhonde, R., & Totey, S. (2011). Chitosan enhances mineralization during osteoblast differentiation of human bone marrow-derived mesenchymal stem cells, by upregulating the associated genes. *Cell Proliferation*, *44*(6), 537–549.

Miller, G. L. (1959). Use of dinitrosalicylic acid reagent for determination of reducing sugar. *Analytical Chemistry*, *31*(3), 426–428.

Muzzarelli, R. A. A. (2009). Chitins and chitosans for the repair of wounded skin, nerve, cartilage and bone. *Carbohydrate Polymers*, *76*(2), 167–182.

Muzzarelli, R. A. A., Greco, F., Busilacchi, A., Sollazzo, V., & Gigante, A. (2012). Chitosan, hyaluronan and chondroitin sulfate in tissue engineering for cartilage regeneration: A review. *Carbohydrate Polymers*, *89*, 723–739. http://dx.doi.org/10.1016/j.carbpol.2012.04.057

Muzzarelli, R. A. A., Terbojevich, M., Muzzarelli, C., & Francescangeli, O. (2002). Chitosans depolymerized with the aid of papain and stabilized as glycosylamines. *Carbohydrate Polymers*, *50*(1), 69–78.

Nam, T., Park, S., Lee, S.-Y., Park, K., Choi, K., Song, I. C., et al. (2010). Tumor targeting chitosan nanoparticles for dual-modality optical/MR cancer imaging. *Bioconjugate Chemistry*, *21*(4), 578–582.

Novoa-Carballal, R., & Muller, A. H. E. (2012). Synthesis of polysaccharide-b-PEG block copolymers by oxime click. *Chemical Communications*, *48*(31), 3781–3783.

Onishi, H., & Machida, Y. (1999). Biodegradation and distribution of water-soluble chitosan in mice. *Biomaterials*, *20*(2), 175–182.

Ottoy, M. H., Varum, K. M., & Smidsrod, O. (1996). Compositional heterogeneity of heterogeneously deacetylated chitosans. *Carbohydrate Polymers*, *29*(1), 17–24.

Qaqish, R., & Amiji, M. (1999). Synthesis of a fluorescent chitosan derivative and its application for the study of chitosan–mucin interactions. *Carbohydrate Polymers*, *38*(2), 99–107.

Rabea, E. I., Badawy, M. E. T., Stevens, C. V., Smagghe, G., & Steurbaut, W. (2003). Chitosan as antimicrobial agent: Applications and mode of action. *Biomacromolecules*, *4*(6), 1457–1465.

Ranaldi, G., Marigliano, I., Vespignani, I., Perozzi, G., & Sambuy, Y. (2002). The effect of chitosan and other polycations on tight junction permeability in the human intestinal Caco-2 cell line. *The Journal of Nutritional Biochemistry*, *13*(3), 157–167.

Sadeghi, A. M. M., Amini, M., Avadi, M. R., Siedi, F., Rafiee-Tehrani, M., & Junginger, H. E. (2008). Synthesis, characterization, and antibacterial effects of trimethylated and triethylated 6-NH_2-6-deoxy chitosan. *Journal of Bioactive and Compatible Polymers*, *23*(3), 262–275.

Schipper, N. G. M., Olsson, S., Hoogstraate, J. A., deBoer, A. G., Vårum, K. M., & Artursson, P. (1997). Chitosans as absorption enhancers for poorly absorbable drugs 2: Mechanism of absorption enhancement. *Pharmaceutical Research*, *14*(7), 923–929.

Şenel, S., Kremer, M. J., Kaş, S., Wertz, P. W., Hıncal, A. A., & Squier, C. A. (2000). Enhancing effect of chitosan on peptide drug delivery across buccal mucosa. *Biomaterials*, *21*(20), 2067–2071.

Takaoka, Y., Tsutsumi, H., Kasagi, N., Nakata, E., & Hamachi, I. (2006). One-pot and sequential organic chemistry on an enzyme surface to tether a fluorescent probe at the proximity of the active site with restoring enzyme activity. *Journal of the American Chemical Society*, *128*(10), 3273–3280.

Thanou, M., Florea, B. I., Geldof, M., Junginger, H. E., & Borchard, G. (2002). Quaternized chitosan oligomers as novel gene delivery vectors in epithelial cell lines. *Biomaterials*, *23*(1), 153–159.

Thygesen, M. B., Munch, H., Sauer, J., Clo, E., Jorgensen, M. R., Hindsgaul, O., et al. (2010). Nucleophilic catalysis of carbohydrate oxime formation by anilines. *Journal of Organic Chemistry*, *75*(5), 1752–1755.

Thygesen, M. B., Sauer, J., & Jensen, K. J. (2009). Chemoselective capture of glycans for analysis on gold nanoparticles: Carbohydrate oxime tautomers provide functional recognition by proteins. *Chemistry – A European Journal*, *15*(7), 1649–1660.

Thygesen, M. B., Sorensen, K. K., Clo, E., & Jensen, K. J. (2009). Direct chemoselective synthesis of glyconanoparticles from unprotected reducing glycans and glycopeptide aldehydes. *Chemical Communications*, (42), 6367–6369.

Yeh, T.-H., Hsu, L.-W., Tseng, M. T., Lee, P.-L., Sonjae, K., Ho, Y.-C., et al. (2011). Mechanism and consequence of chitosan-mediated reversible epithelial tight junction opening. *Biomaterials*, *32*(26), 6164–6173.